JOURNAL OF SEMICONDUCTOR TECHNOLOGY AND SCIENCE, VOL.16, NO.3, JUNE, 2016
http://dx.doi.org/10.5573/JSTS.2016.16.3.255
ISSN(Print) 1598-1657
ISSN(Online) 2233-4866

Full-Wave Rectifier with Vibration Detector for Vibrational Energy Harvesting Systems

Eun-Jung Yoon, Min-Jae Yang, Jong-Tae Park, and Chong-Gun Yu

Abstract—**In this paper, a full-wave rectifier (FWR) with a simple vibration detector suitable for use with vibrational energy harvesting systems is presented. Conventional active FWRs where active diodes are used to reduce the diode voltage drop and increase the system efficiency are usually powered from the output. Output-powered FWRs exhibit relatively high efficiencies because the comparators used in active diodes are powered from the stable output voltage. Nevertheless, a major drawback is that these FWRs consume power from the output storage capacitor even when the system is not harvesting any energy. To overcome the problem, a technique using a simple vibration detector consisting of a peak detector and a level converter is proposed. The vibration detector detects whether vibrational energy exists or not in the input terminal and disables the comparators when there is no vibrational energy. The proposed FWR with the vibration detector is designed using a 0.35-μm CMOS process. Simulation results have verified the effectiveness of the proposed scheme. By using the proposed vibration detector, a decrease in leakage current by approximately 67,000 times can be achieved after the vibration disappears.**

Index Terms—**Full-wave rectifier, vibrational energy, energy harvesting, vibration detector, active diode**

I. INTRODUCTION

Harvesting energy from the environment to power small electronic systems, a process that is known as energy harvesting, has recently attracted considerable research interest [1-3]. Vibrational energy is one of the major energy sources being explored for energy harvesting [2]. This form of energy is usually transduced into electrical energy using piezoelectric (PZT) devices. Because the output of a PZT material is similar to an ac voltage, a rectifier (an ac-dc converter) is required to generate a dc power supply for application loads as shown in Fig. 1. The rectifier must have high conversion efficiency in order to transfer the maximum amount of power from the harvester to the load.

Rectifiers based on simple p-n junctions are usually avoided in CMOS processes. Therefore, full-wave rectifiers (FWRs) are usually realized with MOSFETs. Conventional passive FWRs using four diode-connected MOSFETs [3] or gate cross-coupled rectifiers using two MOS diodes and two MOS switches [4] suffer from diode voltage drop that reduces the available output voltage and thus system efficiency. Thus, active FWRs have been proposed to reduce diode voltage drop and

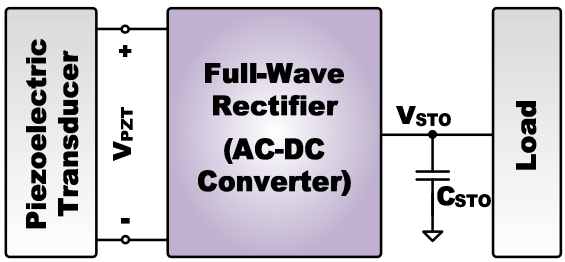

Fig. 1. Block diagram of general vibrational energy harvesting system.

Manuscript received Mar. 31, 2015; accepted Jan. 19, 2016
Dept. of Electronics Engineering, Incheon National University
E-mail : chong@inu.ac.kr

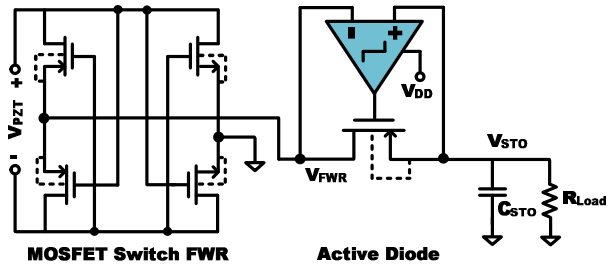

Fig. 2. Two-stage active full-wave rectifier.

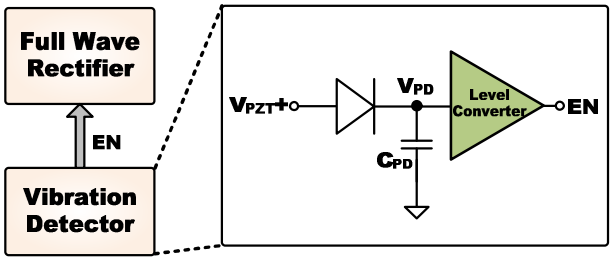

Fig. 3. Proposed FWR with vibration detector.

power loss. Among the various active FWRs, a two-stage implementation as shown in Fig. 2 has been popularly utilized for energy harvesting applications [5-7]. The first stage is an MOSFET switch FWR that converts the negative half wave into a positive half wave with minimized voltage drop and power consumption. This stage cannot charge the storage capacitor (C_{STO}) directly because the current direction cannot be controlled. The possible reverse current is thus blocked by an active diode shown in the second stage of Fig. 2. The second stage consists of a PMOS switch and a comparator. The comparator detects the voltage difference between the two terminals (V_{FWR} and V_{STO}) and determines when to turn the switch on or off.

Two schemes are widely adopted for powering the comparator. In the first scheme [5] the comparator is powered from the input terminal ($V_{DD} = V_{FWR}$), whereas in the other scheme [6, 7], the comparator is powered from the output terminal ($V_{DD} = V_{STO}$). In the input-powered configuration, the comparator consumes power only when the input is sufficiently high. As a result, the rectifier has no standby power consumption when the harvester is not active. The comparator is limited in performance because it is powered from the ac voltage (V_{FWR}). Thus, the peak efficiency of the input-powered rectifier is limited to 82% [5]. In the output-powered configuration, the comparator is powered from the dc voltage (V_{STO}) after start-up, and thus, its performance can be better than that of the input-powered scheme. The output-powered rectifier exhibits a better peak efficiency up to 94% [7]. Nevertheless, output-powered rectifiers have one major drawback when used for energy harvesting systems. They consume power from the storage capacitor even when the system is not harvesting any energy. If there are long periods of inactivity of the harvester, the storage capacitor will be fully discharged.

In this paper, we propose a technique to overcome this problem of output-powered rectifiers employing a simple vibration detector to turn off the comparator when there is no vibrational energy.

II. Circuit Design

The proposed FWR with the vibration detector is shown in Fig. 3. The FWR is the two-stage active rectifier as shown in Fig. 2 where the comparator is powered from the output terminal, but it is designed to have an enable function. A vibration detector is used to disable the comparator when there is not any alternating signal in the input terminal (V_{PZT}). As a result, the rectifier does not consume any power when the harvester is not active.

The vibration detector comprises a simple peak detector and a level converter as shown in Fig. 3. The designed peak detector consists of a p-type diode of size 800 nm × 800 nm and a small capacitor (C_{PD} = 100 fF). As the output of the peak detector V_{PD} is reduced owing to the diode voltage drop, a level converter is employed to recover the degraded signal into a full-scale digital signal. If the harvester is active, the peak detector detects the peak value of an input ac signal (V_{PZT}+), and thus, the output signal 'EN' goes to a 'high' level that enables the comparator. If there is no vibration or the vibration is weak, the capacitor C_{PD} is discharged through the reverse leakage path of the diode, and the signal 'EN' returns to a 'low' level, thus disabling the comparator. Since the capacitance at node V_{PD} is less than 200 fF (C_{PD} + parasitic capacitances), the charge to be discharged is not much. Therefore, the diode leakage path is enough for the discharge, eliminating extra circuits for discharging operation. While it depends on the size of the diode, the estimated equivalent resistance of the leakage path in this

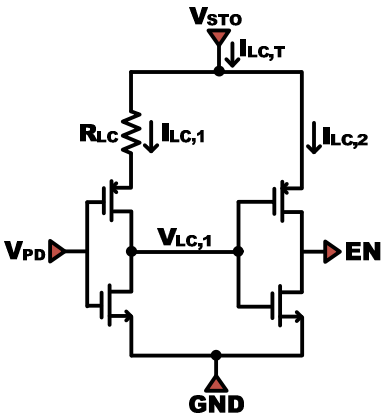

(a)

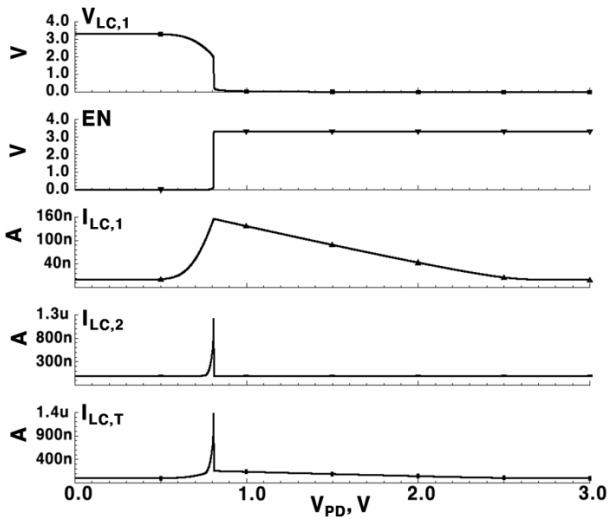

(b)

Fig. 4. (a) Schematic of level converter, (b) DC characteristics when V_{STO} = 3.3 V.

design is about 1 TΩ. Thus, the time constant during discharging is about 200 ms.

The schematic of the level converter and dc characteristics are shown in Fig. 4. The R_{LC} value used in this design is 8 MΩ. The transition point of the level converter is about 800 mV. The peak current of the level converter ($I_{LC,T}$) is 1.38 μA at the transition point, where the first and second stages consumes 155 nA and 1.2 μA, respectively. Therefore, the second stage dominates the leakage current at around transition point. Except for the transition point vicinity, the current of the first stage is dominant. Its average current is 65 nA from 0.5 V to 2.6 V. The simulated transfer curves at different temperatures and process corners are shown in Fig. 5. The transition point is typically 805 mV with a variation of ±50 mV by temperature and process corners.

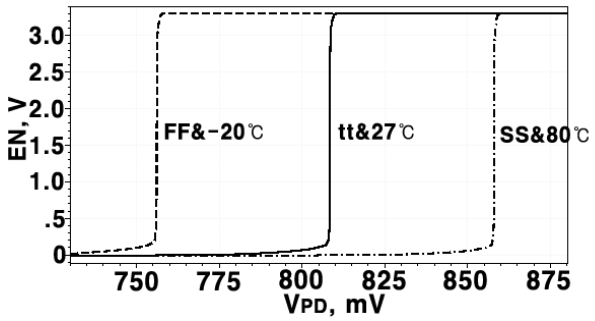

Fig. 5. Transfer curves of level converter at different temperatures and process corners.

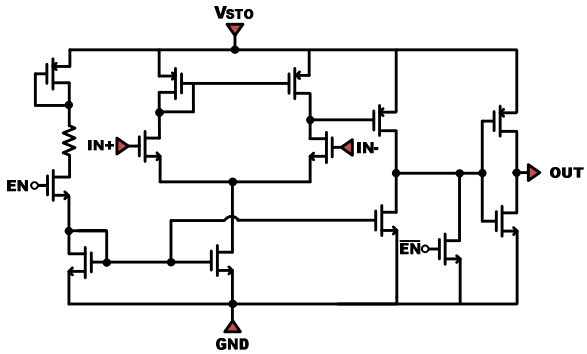

Fig. 6. Schematic of designed comparator with enable switches.

A simple two-stage comparator with enable switches is designed to control the PMOS switch in the active diode. Schematic of the designed comparator with enable switches is shown in Fig. 6. The designed comparator has a dc gain of 80 dB and consumes 2.7 μA from a supply voltage of 3.3 V.

III. SIMULATION RESULTS

The designed FWR is simulated using a 0.35-μm CMOS process. The targeted PZT generator is the Quick Pack QP20W [2] that can generate 125 μW with an acceleration of 7 m/s^2 at 80 Hz. This device can be simply modelled by a current source and parallel capacitor [8]. The amplitude and frequency of the sinusoidal current source are set to 3.3 V and 80 Hz, respectively. The internal parallel capacitor is 0.2 μF. The selected value of the storage capacitor C_{STO} is 47 μF.

Fig. 7 shows the simulated waveforms when the vibration starts at 0 s and stops at 5 s and starts again at 12 s. While the vibration exists, the vibration detector functions and the output signal 'EN' follows V_{STO}, and thus, the comparator is enabled and the FWR output

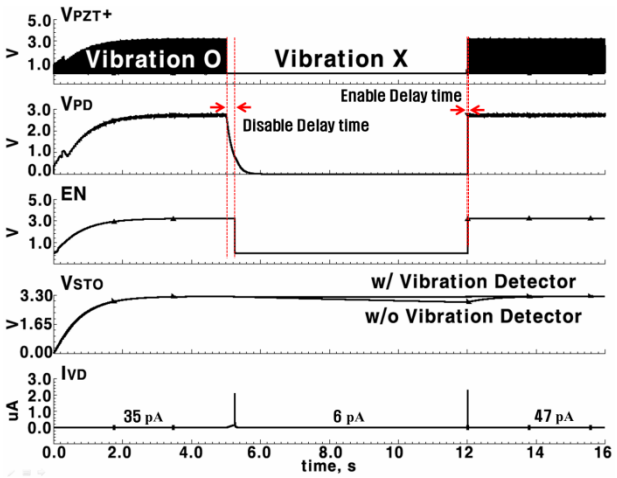

Fig. 7. Simulated waveforms of proposed FWR when the vibration starts at 0 s and stops at 5 s and starts again at 12 s.

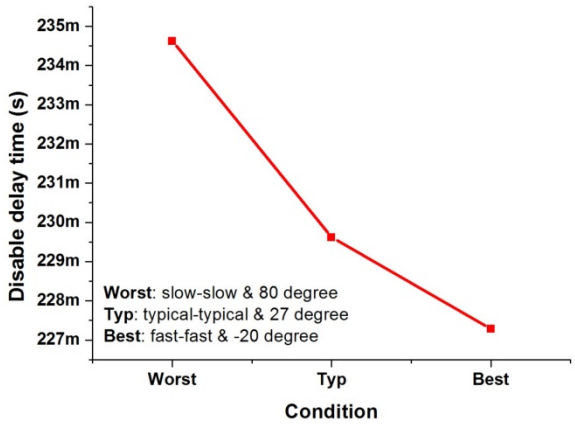

Fig. 8. Disable delay time at different temperatures and process corners.

maintains the peak voltage of the input signal V_{PZT}+. When the vibration disappears at 5 s, the V_{PD} begins to decrease and the 'EN' signal returns to 0 V at the transition point (805 mV) with a disable delay time of 229.6 ms. Therefore, the comparator is disabled and the FWR consumes no power, avoiding the reduction of voltage of V_{STO}, as can be observed in the case of the FWR without a vibration detector. When the vibration starts again at 12 s, the 'EN' signal follows V_{STO} again with an enable delay time of 870 µs. The current consumption of the designed vibration detector (I_{VD}) is very small (dozens of pA) except for the transition points. The peak transition current is about 2.3 µA. As can be seen in Fig. 7, the FWR without a vibration detector consumes power after the vibration disappears, and therefore, V_{STO} decreases gradually. This is because the comparator is not disabled and it consumes power continuously from the storage capacitor. Fig. 8 shows the disable delay time at different temperatures and process corners. As expected, it is related with the RC time constant (~200 ms) in the peak detector.

After the vibration disappears, the leakage currents of the FWR in presence/absence of the vibration detector are compared at different V_{STO} in Fig. 9. The FWR without the vibration detector suffers from relatively large leakage currents due to the current consumption in the comparator. The leakage currents increase with the V_{STO} because the comparator with increased V_{STO} consumes more power. The FWR with the proposed vibration detector is capable of disabling the comparator after the vibration disappears, and thus, the leakage currents are greatly reduced compared with the case when there is no vibration detector. For 80 Hz and 3.3 V, the leakage current of the FWR without the vibration detector is 2.4 µA; however, the leakage current of the FWR with the vibration detector is 36 pA. It can thus be seen that using the proposed vibration detector achieves approximately 67,000 times decrease in leakage current.

The situation should be considered that the vibration suddenly gets weak after the V_{STO} is charged to 3.3 V. When the vibration amplitude decreases from 3.3 V to 0 V~3 V, the leakage currents of the FWR in presence /absence of the vibration detector are compared in Fig. 10. If the vibration amplitude becomes lower than V_{STO} (~3.3 V) and the V_{PD} approaches the transition point (~800 mV) of the level converter, then the leakage current of the FWR can be relatively large (~2 µA). However, in the real environmental vibrations such as human walk, car hood, train floor, microwave oven, and so on, vibration amplitude tends to change every moment [9-11]. Therefore, there is not much chance that the vibration maintains the amplitude (~1.3 V, the diode drop voltage is about 0.5 V) such that the level converter operates at the transition point for long time. When this case (vibration amplitude changes from 3.3 V to 1.3 V) happens, the leakage current of FWR with the vibration detector is 2 µA, while the leakage current of FWR without the vibration detector is 1.6 µA as can be seen in Fig. 10. Except this point, the leakage current of the FWR with vibration detector is similar with that of the FWR without vibration detector when the vibration amplitude becomes greater than this point (from 3.3 V to > 1.3 V). When the vibration amplitude becomes less

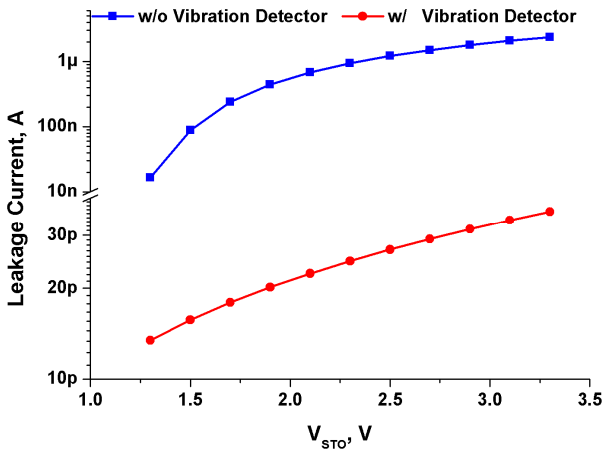

Fig. 9. Leakage currents after vibration disappears for various V_{STO}.

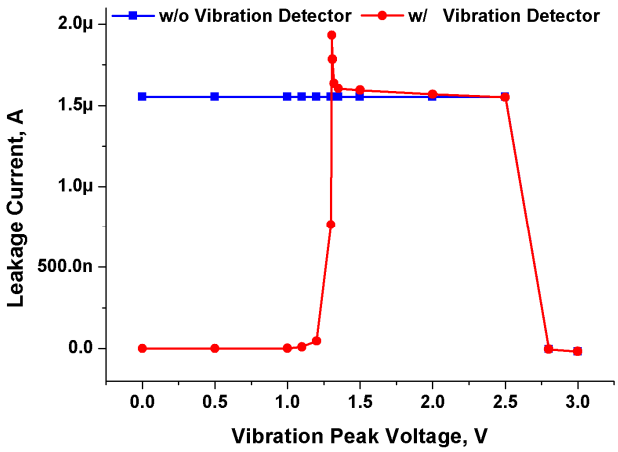

Fig. 10. Leakage currents when the vibration amplitude decreases from 3.3 V to 0 V~3 V.

than this point (from 3.3V to < 1.3 V), the leakage current of the FWR with vibration detector is almost zero while the leakage current of the FWR without vibration detector keep the level of 1.6 µA.

IV. CONCLUSIONS

An FWR with a simple vibration detector consisting of a peak detector and a level converter is presented for energy harvesting applications. The FWR with the proposed vibration detector can disable the comparators in active diodes after vibration disappears, and thus, the leakage currents are greatly reduced compared with the case of the FWR without a vibration detector. Simulation results using a 0.35-µm CMOS process show that an approximate 67,000 times decrease in leakage current can be achieved by using the vibration detector. The proposed scheme can be implemented with a little additional chip area to overcome the major problem of conventional output-powered active FWRs.

ACKNOWLEDGMENTS

This work was supported by the Incheon National University Research Grant in 2014 and was partially supported by IDEC.

REFERENCES

[1] I. Doms, et al, "Capacitive Power Management Circuit for Micropower Thermoelectric Generators With a 1.4 µA Controller," *Solid-State Circuits, IEEE Journal of,* Vol.44, No.10, pp.2824-2833, Oct., 2009.

[2] J. Colomer, et al, "Power-Conditioning Circuitry for a Self-Powered System Based on Micro PZT Generators in a 0.13um Low-Voltage Low-Power Technology," *Industrial Electronics, IEEE Transactions on,* Vol.55, No.9, pp.3249-3257, Sept., 2008.

[3] C. Sauer, et al, "Power harvesting and telemetry in CMOS for implant devices," *Circuits and Systems I, IEEE Transactions on*, Vol.52, No.12, pp.2605-2613, Dec., 2005.

[4] M. Ghovanloo and N. Najafi, "Fully integrated wideband high-current rectifiers for inductively powered devices," *Solid-State Circuits, IEEE Journal of,* Vol.39, No.11, pp.1976-1984, Nov., 2004.

[5] Y. Rao and D. P. Arnord, "An Input-Powered Vibrational Energy Harvesting Interface Circuit With Zero Standby Power," *Power Electronics, IEEE Transactions on,* Vol.26, No.12, pp.3524-3533, Dec., 2011.

[6] C. Peters, et al, "CMOS Integrated Highly Efficient Full Wave Rectifier," *Circuits and Systems, IEEE International Symposium on*, pp.2415-2418, May, 2007.

[7] A. S. Herbawi, et al, "An Ultra-Low-Power Active AC-DC CMOS Converter For Sub-1V Integrated Energy Harvesting Applications," *Sensors, 2013 IEEE*, pp.1-4, 2013.

[8] C. Lu, et al, "Vibration Energy Scavenging System With Maximum Power Tracking for Micropower Applications," *VLSI Systems, IEEE Transactions on*, Vol.19, No.11, pp.2109-2119, Nov., 2011.

[9] I. Neri, et al, "A real vibration database for kinetic energy harvesting application," *Intelligent Material System and Structures*, *Journal of,* Vol.23, No.18, pp.2095-2101, 2012.

[10] Q. Zhu, M. Guan and Y. He, "Vibration Energy Harvesting in Automobiles to Power Wireless Sensors," *Information and Automation, IEEE International Conference on,* pp.349-354, June 2012.

[11] A. Harb, "Energy harvesting: State-of-the-art," *Renewable Energy,* Vol.36, pp.2641-2654, 2011.

Eun-Jung Yoon received the B.S. and M.S. degrees in the Department of Electronics Engineering from Incheon National University, Incheon, Korea, in 2011 and 2013, respectively. She is currently pursuing the Ph.D. degree. Her research interests include micro-scale energy harvesting system design and analog/mixed-mode IC design.

Min-Jae Yang received the B.S. degree in the Department of Electronics Engineering from Incheon National University, Incheon, Korea, in 2014. He is currently pursuing the M.S. degree. His research interests include DC-DC converter design and analog/mixed-mode IC design.

Jong-Tae Park received the B.S. degree in Electronics Engineering from Kyungpook National University, Korea in 1981, and the M.S. and Ph.D. degrees from Yonsei University, Seoul, Korea in 1983 and 1987, respectively, where he performed the device characterization and modeling of SOI CMOS. From 1983 to 1985, he was a Researcher at GoldStar Semiconductor, Inc., Korea, where he worked on the development of SRAM. He joined the Department of Electronics Engineering, Incheon National University, Incheon, Korea in 1987, where he is now a professor. As a Visiting Scientist at Massachusetts Institute of Technology, Cambridge in 1991, he conducted research in hot carrier reliability of CMOS. His research interests are device and circuit design of RF-CMOS and flash memory, circuit design for neuron-chips, and the thin oxide reliability.

Chong-Gun Yu received the B.S. and M.S. degrees in Electronics Engineering from Yonsei University, Seoul, Korea in 1985 and 1987, respectively. He was a graduate student at Texas A&M University, College Station, TX from 1989 to 1991. He received the Ph.D. degree in Electrical and Computer Engineering from Iowa State University, Ames, IA in 1993. He joined the Department of Electronics Engineering, Incheon National University, Incheon, Korea in 1994, and currently serves as Professor. His research interests include analog and mixed-mode IC design.